Title

Deconvolving Glacial Ocean Carbonate Chemistry from the Planktonic Foraminifera Carbon Isotope Record

ISBN

9781461368830

Authors

Spero, Howard J
Bijma, Jelle
Lea, David W
et al.

Publication Date

1999

DOI

10.1007/978-1-4615-4197-4_19

Peer reviewed

19

DECONVOLVING GLACIAL OCEAN CARBONATE CHEMISTRY FROM THE PLANKTONIC FORAMINIFERA CARBON ISOTOPE RECORD

Howard J. Spero[1], Jelle Bijma[2], David W. Lea[3], and Ann D. Russell[1]

[1]Department of Geology
University of California Davis
Davis, California 95616, U.S.A.

[2]Department of Geology
University of Bremen
P. O. Box 330 440, D-28334 Bremen
Germany

[3]Department of Geological Sciences and
the Marine Science Institute
University of California Santa Barbara
Santa Barbara, California 93106
U.S.A.

1. INTRODUCTION

Among the most important challenges remaining to be addressed by Quaternary paleoceanographers is the mechanism responsible for lower pCO_2 during the Last Glacial Maximum (LGM). One of the more widely accepted clues for this mechanism is the observation that the carbon isotopic composition ($\delta^{13}C$) of glacial planktic and benthic foraminifera was more negative relative to the Holocene (Curry and Crowley, 1987; Shackleton, 1977; Shackleton *et al.*, 1992). It has been shown that the $\delta^{13}C$ of a foraminiferal shell is a function of the $\delta^{13}C$ of dissolved inorganic carbon (ΣCO_2) (Spero, 1992). Although physiological processes such as symbiont photosynthesis and respiration can also influence shell $\delta^{13}C$ (Bijma *et al.*, 1998a; Bijma *et al.*, 1999; Spero *et al.*, 1991), the practice of analyzing multiple shells from each interval in a core should average out these vital effects. Hence, lower glacial $\delta^{13}C$ values are thought to reflect changes in mean ocean $\delta^{13}C$ (Shackleton, 1977).

Based on this premise, a number of researchers have proposed that reduced glacial $\delta^{13}C$ values were due to the transfer and remineralization of ^{12}C-rich terrestrial organic

Reconstructing Ocean History: A Window into the Future
edited by Abrantes and Mix, Kluwer Academic / Plenum Publishers, New York, 1999.

matter to the glacial ocean-atmosphere reservoir (Crowley, 1995; Shackleton, 1977). Estimate of the change in mean ocean $\delta^{13}C$ based on benthic foraminifera records is –0.32‰ (Boyle, 1992; Curry *et al.*, 1988; Duplessy *et al.*, 1988; Matsumoto and Lynch-Stieglitz, 1999). Such a value would suggest that approximately 5×10^{17} g (500 Gt) of carbon were removed from the continents during the LGM. Alternative estimates based on pollen databases suggest decreases of 750–1,350 Gt of carbon in the terrestrial biosphere at the LGM (Crowley, 1995). If all this carbon were remineralized, the glacial-interglacial (G-I) $\delta^{13}C$ difference should have been even greater.

Recently, Spero *et al.* (1997) demonstrated a second mechanism to lower shell $\delta^{13}C$ values. Laboratory experiments conducted on the living planktonic foraminifers *Orbulina universa* and *Globigerina bulloides* demonstrated that both $\delta^{13}C$ and $\delta^{18}O$ values decrease with increasing seawater carbonate ion concentration ($[CO_3^{2-}]$) or pH. Both theoretical considerations (Archer and Maier-Reimer, 1994; Broecker and Peng, 1987; Lea *et al.*, 1999) and geochemical data in the form of boron isotope ($\delta^{11}B$) measurements (Sanyal *et al.*, 1997; Sanyal *et al.*, 1995) suggest that regions of the glacial ocean were more alkaline than today. Therefore, elevated surface water pH should produce foraminifera shells with lower $\delta^{13}C$ values without altering mean ocean $\delta^{13}C$. Lea *et al.* (1999) explored to what extent planktonic carbon isotope records could be explained by a carbonate ion influence. They concluded that glacial $\delta^{13}C$ values are compatible in magnitude with the calculated influence of higher glacial carbonate ion, but the difference in timing between tropical/sub-tropical $\delta^{13}C$ records and predicted change in surface water carbonate ion appears to preclude carbonate ion concentrations as the principal control on shell $\delta^{13}C$. A key to interpreting the foraminiferal $\delta^{13}C$ record is to incorporate an unequivocal method of deconvolving the carbonate ion effect from that of the change in dissolved inorganic carbon (DIC) $\delta^{13}C$ due to mean ocean change and other potential influences such as changing the strength of the biological pump.

Reconstructions of tropical sea surface conditions during the late Quaternary have relied primarily on the stable isotope geochemistry of two species of planktonic foraminifera, *Globigerinoides sacculifer* and *G. ruber*. Generally, both species have similar depth and seasonal distributions (Deuser, 1987; Deuser and Ross, 1989; Fairbanks *et al.*, 1982; Ravelo and Fairbanks, 1992; Thunell *et al.*, 1983) and are constrained to the surface photic zone because of their obligate association with symbiotic dinoflagellates. Because of these similarities, researchers have used the two species interchangeably in hundreds of studies to reconstruct glacial ice volume records and estimate sea surface temperature variations from shell $\delta^{18}O$ values. Whereas the *G. sacculifer* records typically exhibit a maximum G-I $\delta^{13}C$ difference of -0.24 ± 0.12‰ (Curry and Crowley, 1987), the published *G. ruber* records suggest the G-I $\delta^{13}C$ offset may be two to three times as large (Lea *et al.*, 1999). If both species record mean ocean $\delta^{13}C$ change equally (as expected from their similarities), then this difference could be explained by a different geochemical response to changes in the carbonate chemistry of seawater (Lea *et al.*, 1999).

In this paper, we utilize a new suite of experimental data (Bijma *et al.*, 1998b) which demonstrates that the $\delta^{13}C$:$[CO_3^{2-}]$ slope relationship for *G. ruber* is nearly twice as large as in *G. sacculifer*. Because shell $\delta^{13}C$ values of the two species should be affected equally by changes in mean ocean $\delta^{13}C$, and the species have different carbonate ion relationships, it may be possible to deconvolve the foraminiferal $\delta^{13}C$ record to calculate the change in surface $[CO_3^{2-}]$ and $\delta^{13}C_{\Sigma CO_2}$ through time. Application of a new set of relationships to a Late Quaternary carbon isotope data set from equatorial Indian Ocean core ODP 714A suggests that surface water $[CO_3^{2-}]$ may have been higher during the LGM and that the sign and magnitude of $\delta^{13}C_{\Sigma CO_2}$ change differ from what is directly indicated by the downcore records.

2. METHODOLOGY

Fossil *G. ruber* (white variety) and *G. sacculifer* (w/o sac) were obtained from the upper 4.5 m of ODP core 714A from the equatorial Indian Ocean (5°N, 74°E). The core was collected from a depth of 2,195 m and has a sedimentation rate of approximately 3.5 cm/kyr through the upper 19 m of the core (Droxler *et al.*, 1990). The original *G. sacculifer* $\delta^{18}O$ and $\delta^{13}C$ data set of Droxler *et al.* (1990) was augmented with additional analyses of both *G. sacculifer* and *G. ruber* (300–355 μm sieve fraction) to obtain samples every 10 cm through the penultimate glacial cycle. The SPECMAP tuned age model used by Droxler *et al.* (1990) is applied here to estimate sediment age. Shells were cleaned of adhering sediment in a sonication bath and 10 shells/sample were pooled in each sample and roasted at 375 °C *in vacuo*, then analyzed with a Fisons Optima IRMS using an Isocarb common acid bath autocarbonate system at 90 °C. Data are presented in per mil (‰) notation relative to the V-PDB standard (unless noted otherwise) where:

$$\delta^{18}O(\text{or } \delta^{13}C) = [(^{18}O/^{16}O_{smpl}/^{18}O/^{16}O_{std}) - 1] \times 1{,}000$$

Analytical precision of the $\delta^{18}O$ and $\delta^{13}C$ measurements is ±0.08 and ±0.05‰ respectively.

3. THE MODEL

The experimental results of Bijma *et al.* (1998b) show that the $\delta^{13}C$ and $\delta^{18}O$ values of *G. sacculifer* and *G. ruber* decrease with increasing seawater $[CO_3^{2-}]$ (and pH). The slopes of the $\delta^{13}C/[CO_3^{2-}]$ relationships are −0.0047 ± 0.001 and −0.0089 ± 0.001‰ per μmol/kg (±2σ) and $\delta^{18}O/[CO_3^{=}]$ are −0.0014 ± 0.0003 and −0.0022 ± 0.0006‰ per μmol/kg for *G. sacculifer* and *G. ruber* respectively. These relationships are within the range of our earlier experimental results on *O. universa* and *G. bulloides* (Spero *et al.*, 1997) (Table 1), demonstrating that the slopes of the carbonate ion effect (CIE) are species specific.

Because the slopes of the *G. sacculifer* and *G. ruber* $[CO_3^{2-}]$:$\delta^{13}C$ relationships are significantly different, it should be possible to separate the influence of carbonate ion from changing mean ocean $\delta^{13}C$ at a given location if certain inferences and assumptions are true. For instance both species possess symbiotic dinoflagellates (Anderson and Bé, 1976; Lee *et al.*, 1965) and therefore live in the photic zone. Furthermore, *G. sacculifer* and *G. ruber* share the same general seasonal and mixed layer habitat (Fairbanks *et al.*, 1980; Ravelo and Fairbanks, 1992; Tolderlund and Bé, 1971) so isotope values obtained from multi-shell analyses should yield data that reflect a similar season and depth mean.

Our most critical assumption regards the environment of final calcite addition for

Table 1. Experimentally derived slopes for planktic foraminifera carbonate ion effect

Species	$\delta^{13}C/[CO_3^{2-}]$*	$\delta^{18}O/[CO_3^{2-}]$*	Reference
Orbulina universa	−0.0058†	−0.0020†	Spero *et al.* (1997)
Globigerina bulloides	−0.0130†	−0.0045†	Spero *et al.* (1997)
Globigerinoides sacculifer	−0.0047	−0.0014	Bijma *et al.* (1998)
Globigerinoides ruber	−0.0089	−0.0022	Bijma *et al.* (1998)

*units are ‰ $\mu mol^{-1}\ kg^{-1}$.

†slopes are averages of all experiments.

the two species. It is well known that *G. sacculifer* adds a veneer of gametogenic calcite at the end of its life cycle just prior to reproduction (Bé, 1980; Duplessy *et al.*, 1981). Bé (1980) estimated that as much as 28% of the shell mass could be added during this calcification event and mass balance calculations place the gametogenic calcification depth in the upper seasonal thermocline below the primary calcification depth range (Lohmann, 1995). In contrast, *G. ruber* does not add gametogenic calcite so its shell calcite reflects mixed layer chemistry alone (Caron *et al.*, 1990). In the following discussion, we assume that the carbon chemistry of seawater (e.g., $\delta^{13}C_{\Sigma CO2}$ and $[CO_3^{2-}]$) in the tropical Indian Ocean (mixed layer depth ~ 50 m) is constant across the full calcification depth of the two species (maximum depth for *G. sacculifer* is ~ 100 m).

Given the above assumption and inferences, we can draw two conclusions about shells collected from the sedimentary record. First, if both species are affected equally by bioturbation, and dissolution is similar for both, then the $\delta^{13}C$ of *G. sacculifer* and *G. ruber* from any interval in a core should record $\delta^{13}C_{\Sigma CO2}$ equally (Spero, 1992). Second, if a number of shells are analyzed from each interval, the effect of intershell differences due to symbiont photosynthesis as it varies within the light field of the photic zone (Bijma *et al.*, 1992; Billups and Spero, 1995; Spero and Lea, 1993; Spero and Williams, 1989) should average out and the interspecific $\delta^{13}C$ offset (vital effect) that is observed between the two species in the core top interval should remain constant through time. We address potential issues with these assumptions later in the paper.

With the above two caveats, it is possible to solve for downcore changes in surface $[CO_3^{2-}]$ and $\delta^{13}C_{\Sigma CO2}$ using the differential response of *G. ruber* and *G. sacculifer* to changes in surface $[CO_3^{2-}]$. Given that downcore shifts in the $\delta^{13}C$ of these two species can be described as a function of the $\delta^{13}C_{\Sigma CO2}$ and surface $[CO_3^{2-}]$, then at any time (or interval) "t":

$$(\delta^{13}C_{sacc})_t = \delta^{13}C_{\Sigma CO2} + m_{sacc} * [CO_3^{2-}]_t \quad (1)$$

and

$$(\delta^{13}C_{ruber})_t = \delta^{13}C_{\Sigma CO2} + m_{ruber} * [CO_3^{2-}]_t \quad (2)$$

where $m_{ruber} = -0.0089‰\,\mu mol^{-1}\,kg^{-1}$ and $m_{sacc} = -0.0047‰\,\mu mol^{-1}\,kg^{-1}$.

Species specific "vital effects" which result from the differential influence of symbiont photosynthesis (among other physiological processes) on shell $\delta^{13}C$ creates an offset which is specific for a given geographical region. Assuming this "vital effect" is constant within a core, we can correct for the offset between *G. ruber* and *G. sacculifer* using:

$$(\delta^{13}C_{ruber})_t = \delta^{13}C_{\Sigma CO2} + m_{ruber} * [CO_3^{2-}]_t + v \quad (3)$$

where "v" is the "vital effect" difference between the two species, and is estimated by:

$$v = (\delta^{13}C_{sacc} - \delta^{13}C_{ruber})_{\text{core top}} \quad (4)$$

If "v" is subtracted from all paired ($\delta^{13}C_{sacc} - \delta^{13}C_{ruber}$) differences throughout the core, we obtain a suite of down core difference values which are corrected for "vital effects", according to the simple assumption of constant vital effect offsets through time:

$$(\delta^{13}C_{sacc} - \delta^{13}C_{ruber})_{t-ct} = (\delta^{13}C_{sacc} - \delta^{13}C_{ruber})_{t} - (\delta^{13}C_{sacc} - \delta^{13}C_{ruber})_{ct} \quad (5)$$

and can solve for the change in $[CO_3^{2-}]$ between the core top and any interval "t" downcore, $\Delta[CO_3^{2-}]_{t-ct}$, where

$$(\delta^{13}C_{sacc} - \delta^{13}C_{ruber})_{t-ct} = \Delta[CO_3^{2-}]_{t-ct} * (m_{sacc} - m_{ruber}) \quad (6)$$

and

$$\Delta[CO_3^{2-}]_{t-ct} = (\delta^{13}C_{sacc} - \delta^{13}C_{ruber})_{t-ct} / (m_{sacc} - m_{ruber}) \quad (7)$$

Here, $m_{sacc} - m_{ruber} = 0.0042\,\mu mol^{-1}\,kg^{-1}$, the difference in $\delta^{13}C$ response to carbonate ion between the species.

Once $\Delta[CO_3^{2-}]_{t-ct}$ is calculated, $\Delta\delta^{13}C_{\Sigma CO2}$ is determined relative to the core top from either (1) or (2) where:

$$\Delta\delta^{13}C_{\Sigma CO2} = (\Delta\delta^{13}C_{sacc})_{t-ct} - m_{sacc} * \Delta[CO_3^{2-}]_{t-ct} \quad (8)$$

or

$$\Delta\delta^{13}C_{\Sigma CO2} = (\Delta\delta^{13}C_{ruber})_{t-ct} - m_{ruber} * \Delta[CO_3^{2-}]_{t-ct} \quad (9)$$

4. DOWNCORE RECONSTRUCTIONS OF $\Delta[CO_3^{2-}]$ AND $\Delta\delta^{13}C_{\Sigma CO2}$

Core ODP 714A is located to the west of GEOSECS station 447. Hydrographic and shorebased data from the water column at station 447 show that the mixed layer is at least 50 m deep, with a SST of 30.0 °C and $\delta^{13}C_{\Sigma CO2}$ = 1.56‰ during the April 1978 cruise. Although only ΣCO_2 data are available for this site (1909 µmol/kg), if we assume that the surface waters were in approximate equilibrium with the atmosphere (pCO_2 = 350 µatm), then the calculated $[CO_3^{2-}]$ would be 246 µmol/kg which is similar to the surface ocean $[CO_3^{2-}]$ near Puerto Rico where the experiments in Bijma *et al.* (1998) were conducted.

The *G. sacculifer* and *G. ruber* $\delta^{18}O$ stratigraphies (Fig. 1a) show a normal G-I cycle with a prominent Stage 1/2 transition and clearly discernible stage 3, 4, 5c and 5e peaks. Only stage 5a appears to be weakly defined. Unlike the oxygen isotope data, the $\delta^{13}C$ stratigraphy (Fig. 1b) for the two species displays little apparent Milankovich frequency across the 130 kyr record. Rather, we observe a series of high frequency oscillations which clearly differ in sign and magnitude between the two species. To better visualize this difference, we have smoothed both $\delta^{13}C$ data sets using a 3-point running mean (Fig. 1c).

In Figs. 1b and 1c, the difference between the two $\delta^{13}C$ records is very apparent. Whereas *G. sacculifer* records a typical ≈ –0.20‰ G-I $\delta^{13}C$ difference, *G. ruber* records a –0.6‰ change. In reality, the –0.2‰ G-I difference is not between the LGM and Holocene, but rather between the deglacial and Holocene (Curry and Crowley, 1987). A clear $\delta^{13}C$ maximum can be seen between 20 and 25 kyr in the *G. sacculifer* $\delta^{13}C$ values. Although a similar maximum is also observed in the *G. ruber* record, it lags the *G. sacculifer* record and does not exceed Holocene $\delta^{13}C$ values as does the *G. sacculifer*

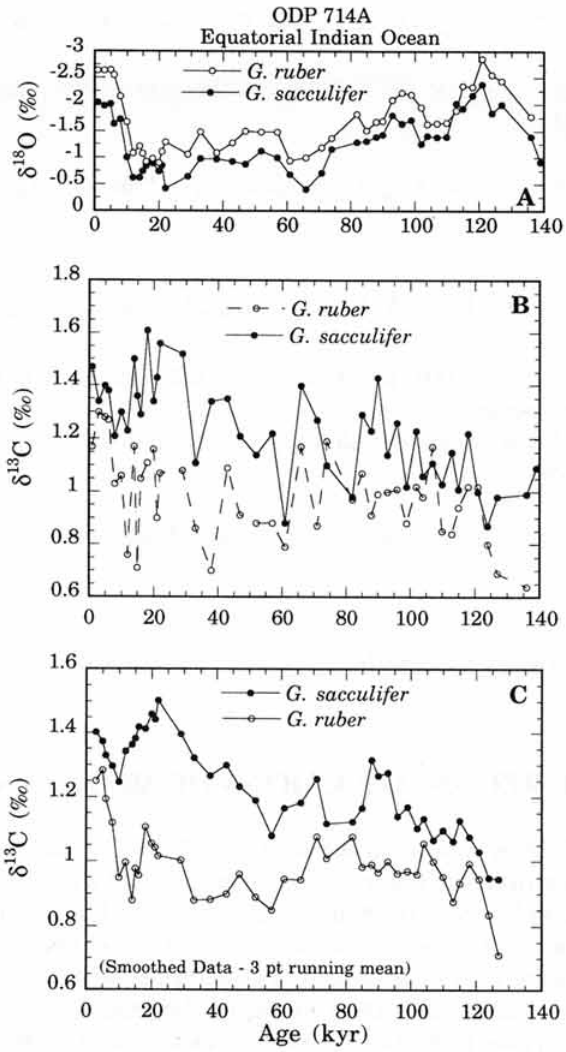

Figure 1. Equatorial Indian Ocean core ODP 714A stable isotope stratigraphy. (a) *G. sacculifer* and *G. ruber* $\delta^{18}O$ values. (b) *G. sacculifer* and *G. ruber* $\delta^{13}C$ values. Stable isotope data include data from Droxler *et al.* (1990) augmented by additional measurements made in this study; (c) $\delta^{13}C$ stratigraphies smoothed with a 3-point running mean.

glacial signal. Similar offsets in both timing and magnitude between the two species can be traced throughout the last 130 kyr. If *G. sacculifer* and *G. ruber* coexist in the same region of the water column and are only tracking $\delta^{13}C_{\Sigma CO_2}$, these differences are difficult to reconcile.

Equation (7) demonstrates that the difference between the *G. ruber* and *G. sacculifer* $\delta^{13}C$ records should be a function of surface ocean $[CO_3^{2-}]$. After correcting the full (unsmoothed) data set for the core top offset between the species as discussed in the last section, we obtain the reconstructed $\Delta[CO_3^{2-}]$ record in Fig. 2a. Examining the broader pattern from this reconstruction, and ignoring the single point high frequency oscillations, what emerges is: 1) a broad LGM $\Delta[CO_3^{2-}]$ maximum of approximately 50 μmol/kg;

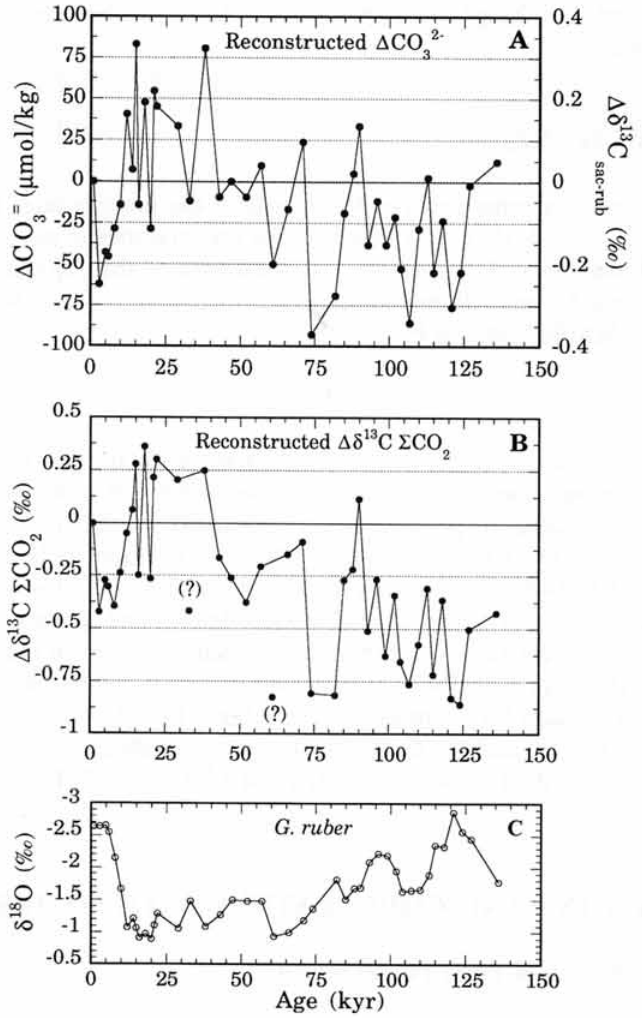

Figure 2. Deconvolved *G. sacculifer* and *G. ruber* carbon isotope records based on the complete $\delta^{13}C$ data set. (a) $\Delta[CO_3^{2-}]$ and calculated $\Delta\delta^{13}C_{sacc\text{-}ruber}$ relative to the core top. (b) Calculated surface water $\Delta\delta^{13}C_{\Sigma CO2}$ relative to the core top. (c) *G. ruber* $\delta^{18}O$ stratigraphy. $\Delta[CO_3^{2-}]$ and $\Delta\delta^{13}C_{\Sigma CO2}$ have been determined using equations described in the text.

2) a gradual reduction in surface $\Delta[CO_3^{2-}]$ to $-60\,\mu mol/kg$ from the start of the deglaciation through the mid-Holocene; 3) oscillating Stage 5a–5e $[CO_3^{2-}]$ which are comparable to $[CO_3^{2-}]$ concentrations during the Holocene; 4) a $\Delta[CO_3^{2-}]$ minimum of $-90\,\mu mol/kg$ during Stage 4; 5) Late Holocene-like $[CO_3^{2-}]$ concentrations during Stage 3; and, 6) an increase in $[CO_3^{2-}]$ during the Late Holocene.

Deconvolving the surface $\delta^{13}C_{\Sigma CO2}$ record from the influence of seawater $[CO_3^{2-}]$ using either eqs. (8) or (9), yields a broad $\Delta\delta^{13}C$ maximum at the LGM that is between 0.25 and 0.3‰ *higher* than the core top (Fig. 2b). Surface $\delta^{13}C$ decreases during the deglaciation into the mid-Holocene after which values increase at the Late Holocene. A clear $\Delta\delta^{13}C$ minimum correlates with parts of stages 5a and 4. Interestingly, most of the

penultimate interglacial (Stage 5) yields surface $\delta^{13}C$ values that are considerably lower than the Holocene.

5. ERROR ANALYSIS

We performed an error analysis to determine the uncertainties in the calculated parameters ($\Delta[CO_3^{=}]$ and $\Delta\delta^{13}C_{\Sigma CO2}$) based on the uncertainties in m_{sacc} and m_{ruber} and in the measured down-core $\delta^{13}C_{sacc}$ and $\delta^{13}C_{ruber}$. We estimated the one sigma standard deviation (1σ) that we achieved with our samples (in which 10 individuals were pooled) using the approach of Schiffelbein and Hills (1984):

$$\sigma^2_T = \sigma^2_M + \sigma^2_p/n$$

where σ^2_T is total variance, σ^2_m is the machine variance (0.0025‰^{2}; ie $\sigma_M = 0.05$‰), σ^2_p is the estimated population variance, and n is the number of individuals pooled in the sample (10). We estimated the population variance for *G. sacculifer* ($\sigma^2_P = 0.1681$‰^{2}) and *G. ruber* ($\sigma^2_P = 0.0961$‰^{2}) by analyzing 22–24 shells of each in Holocene and 22 kyr samples from OPD 714A. The variance for Holocene and 22 kyr samples was the same. The $1\sigma_T$ for our samples of 10 pooled individuals determined this way were ±0.14‰ (*G. sacculifer*) and ±0.11‰(*G. ruber*). We then propagated the errors in the calculated values of $\Delta[CO_3^{=}]$ and $\Delta\delta^{13}C_{\Sigma CO2}$ using the analytical expressions in Bevington (1969) (pp. 60–62), with mean and $1\sigma_T$ values for 10 shells given in Table 2. Finally, we estimate the minimum feasible errors in $\Delta[CO_3^{=}]$ and $\Delta\delta^{13}C_{\Sigma CO2}$, assuming that 50 shells are analyzed per sample. With this assumption, the 1σ error in $\Delta[CO_3^{=}]$ and $\Delta\delta^{13}C_{\Sigma CO2}$ at 22 kyr is ±40 µmol/kg and ±0.23‰ respectively.

6. IMPLICATIONS AND CORRELATION WITH OTHER PROXIES

6.1. Surface $\Delta\delta^{13}C$ and Dust Fertilization

Given that this is our first attempt to apply these relationships to the fossil record, and given the relatively large potential errors estimated above, it is premature to view these reconstructions as strict quantitative estimates. If our deconvolution is correct, we are left with two interesting conclusions about the equatorial Indian Ocean during the LGM; surface water $\delta^{13}C$ and $[CO_3^{2-}]$ were higher than during the Holocene. The conclusion that LGM surface ocean $[CO_3^{2-}]$ was elevated is not new. Rather, it is a necessary chemical state of the ocean (Broecker, 1982; Lea *et al.*, 1999) given that the ocean surface is essentially in equilibrium with the atmosphere over long time periods and that LGM pCO_2 was approximately 80 µatm lower than during the Holocene (Barnola *et al.*, 1987).

Table 2. Results from error analysis (using only 10 shells/sample)

Age (kyr)	Mean $\delta^{13}C_{sacc}$ (‰)	Mean $\delta^{13}C_{ruber}$ (‰)	$\Delta[CO_3^{=}] \pm 1\sigma$ (µmol/kg)	$\Delta\delta^{13}C_{\Sigma CO2} \pm 1\sigma$ (‰)
0	1.47 ± 0.14	1.17 ± 0.11		
22	1.43 ± 0.14	0.90 ± 0.11	55 ± 63	0.22 ± 0.36
74	1.10 ± 0.14	1.19 ± 0.11	−93 ± 68	−0.81 ± 0.39

Recent boron isotope data by Sanyal *et al.* (1995), which demonstrated higher sea surface pH during the LGM, further supports this hypothesis and our conclusion.

The reconstruction from ODP 714A indicates that surface water $\delta^{13}C_{\Sigma CO2}$ was more positive during the LGM (Fig. 2b). This result is unexpected yet intriguing in light of the recent hypothesis by Broecker and Hender son (1998) that iron (dust) fertilization may have played a key role in the proliferation of nitrogen fixing cyanobacteria in the subtropics during the LGM. This hypothesis is an extension of the earlier hypothesis of Martin (1990) who proposed that high latitude surface ocean productivity is limited by iron deficiency and therefore phytoplankton cannot take advantage of the nutrients that remain in the photic zone after Fe depletion. Martin argued that the elevated dust flux to the ocean during the LGM could have increased surface productivity in high nutrient low chlorophyll areas, thereby providing a mechanism to reduce atmospheric CO_2. Because surface water $\delta^{13}C$ is controlled by the biological cycling of ^{13}C-depleted organic matter between the shallow, intermediate and deep zones of the ocean (Kroopnick, 1985) an increase in surface productivity due to dust fertilization should correlate with an increase in the $\delta^{13}C$ of surface waters.

During the LGM, the northwestern Indian Ocean received a significant flux of eolian material from the arid regions of Arabia. Mass accumulation rate (MAR) data from piston core RC27–61 in the Arabian Sea (Clemens and Prell, 1990) indicate that eolian fluxes peaked during the LGM, accumulating at a rate of approximately 2 mg/cm^2/yr. Based on isopleth interpolation (Duce *et al.*, 1991) the flux of mineral aerosols to the equatorial waters above ODP 714A is only 3–4 times lower than the MAR at RC27–61. Therefore it is reasonable to assume that the LGM eolian flux at Site 714A increased proportionately with the MAR at RC27–61.

Could the tropical Fe fertilization hypothesis of Broecker and Henderson (1998) explain the $\delta^{13}C$ increase we observe in our reconstruction? A plot of the RC27–61 eolian MAR record with the reconstructed Site 714A $\Delta\delta^{13}C_{\Sigma CO2}$ record (Fig. 3a) shows reasonable agreement between the LGM eolian peak and $\delta^{13}C_{\Sigma CO2}$ maxima although the initial increase in $\Delta\delta^{13}C_{\Sigma CO2}$ clearly leads the MAR record. Maxima in $\Delta\delta^{13}C_{\Sigma CO2}$ during stage 4 and possibly stage 5b are associated with increased eolian MAR although these correlations are more tenuous. Finally, we point out that the hypothesis of Broecker and Henderson may require further evaluation. Recent simulations with a coupled ocean general circulation and sedimentary diagenesis model suggest that carbonate compensation would eliminate all of the pCO_2 drop generated by increased mean ocean nitrate (Archer *et al.*, in press).

6.2. Surface $\Delta[CO_3^{2-}]$ and the Dissolution Record

Variations in surface $[CO_3^{2-}]$ are intimately related to the balance between the supply of alkalinity to surface waters via runoff from the continents, erosion of exposed carbonate platforms during sea level low stands, precipitation and export of $CaCO_3$ shells from super saturated surface waters and changes in the strength of the biological pump. In contrast, the $[CO_3^{2-}]$ of the deep ocean is a function of the age of the deep water and surface supply and subsequent dissolution of sinking $CaCO_3$ shells. Peterson and Prell (1985) examined equatorial Indian Ocean carbonate preservation in core V34–53 (6°S, 89.5°E), along 90°E ridge, southwest of site 714A. Their composite dissolution index (CDI) based primarily on foraminiferal shell fragmentation, shows a stage 4 preservation minimum and stage 2 maximum (Fig. 3b). Our reconstruction of glacial surface water $[CO_3^{2-}]$ change appears to track deep ocean dissolution at V34–53. Because surface and

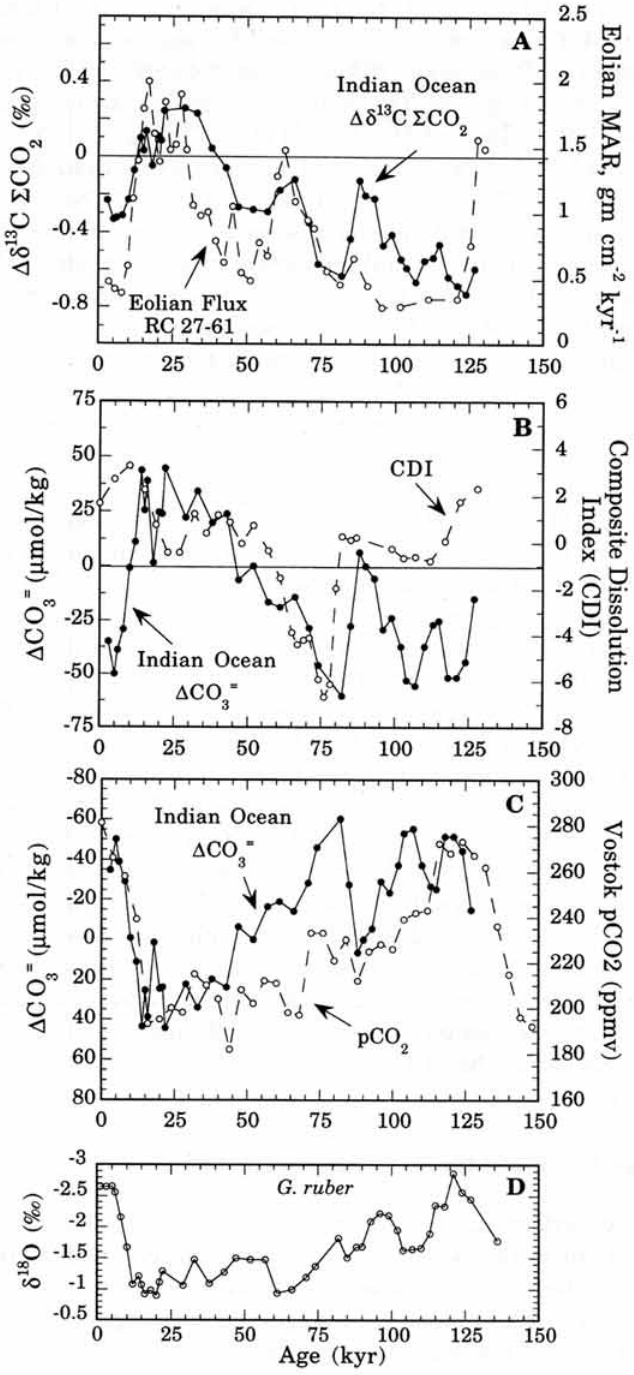

Figure 3. (a) Smoothed (3-pt running mean) $\Delta\delta^{13}C_{\Sigma CO2}$ reconstruction versus eolian mass accumulation rate record from northwestern Indian Ocean core RC27–61 (data from Clemens and Prell (1990)); (b) Smoothed (3-pt running mean) $\Delta[CO_3^{2-}]$ reconstruction plotted with Composite Dissolution Index from equatorial Indian Ocean core V34–53 (data from Peterson and Prell (1985)); (c) Smoothed $\Delta[CO_3^{2-}]$ reconstruction plotted with Vostok pCO_2 record interpolated to 4 kyr intervals (Barnola *et al.*, 1987; Jouzel *et al.*, 1993); (d) *G. ruber* $\delta^{18}O$ stratigraphy.

deep ocean circulation and carbonate chemistry are linked through high latitude convection, and the readjustment time for deep ocean $[CO_3^{2-}]$ change is on the order of 5–10 kyr (Broecker and Peng, 1998), the covariance of the CDI and $[CO_3^{2-}]$ reconstruction suggests that our deconvolving technique could have captured a linkage between surface and deep $[CO_3^{2-}]$ for this region of the Indian Ocean.

Unlike the agreement between the glacial CDI and $[CO_3^{2-}]$ reconstruction, the interglacial CDI and surface $[CO_3^{2-}]$ reconstruction diverge considerably. Specifically, the CDI shows good carbonate preservation whereas the surface record indicates a $[CO_3^{2-}]$ minimum during the Holocene and oscillations with distinct minima between stages 5a and 5e. Given the errors in the $[CO_3^{2-}]$ reconstruction, it is premature to try to reconcile these differences. We are currently working on analyses of *G. ruber* and *G. sacculifer* in nearby cores to confirm the structure and robustness of the reconstructions.

6.3. Surface $\Delta[CO_3^{2-}]$ and the Vostok pCO_2 Record

A direct way to evaluate the surface $[CO_3^{2-}]$ reconstruction for ODP Site 714A is to compare it with the Antarctic Vostok ice core atmospheric pCO_2 record (Barnola *et al.*, 1987). Because the pCO_2 of the sea surface and atmosphere are in approximate equilibrium, changes in atmospheric CO_2 recorded in ice cores must be matched by changes in surface $[CO_3^{2-}]$ (Broecker, 1982; Lea *et al.*, 1999). In general, the surface ocean pCO_2 of tropical and subtropical regions of the ocean with deep mixed layers (such as the water column above Site 714A) should be close to equilibrium with the atmosphere (Takahashi *et al.*, 1997). For instance, the pCO_2 of surface waters to the east of Site 714A (5°N, 90°E) are only 10% higher than atmospheric pCO_2 (367 ppm vs 333 ppm) (Murphy *et al.*, 1994).

The weak agreement between the ODP Site 714A seawater $[CO_3^{2-}]$ reconstruction and Vostok pCO_2 record (Fig. 3c) does not allow us to directly confirm the validity of the deconvolution technique. This creates a dilemma when interpreting our reconstructed $[CO_3^{2-}]$ record. Whereas it can be argued that the $[CO_3^{2-}]$ reconstruction for the penultimate interglacial and LGM through Holocene transition tracks ice core pCO_2, the oscillations during Stage 5 and apparent lag in surface $[CO_3^{2-}]$ change relative to ice core pCO_2 are inconsistent with surface waters that are close to equilibrium with the atmosphere. One possibility is that the tropical Indian Ocean between Stage 2 and Stage 5e was shifting between disequilibrium and equilibrium states via changes in the strength of the biological pump, surface $CaCO_3$ production and the local supply of CaO and alkalinity (CO_3^{2-} and HCO_3^-) via erosion and runoff from the Himalyan plateau and exposed Indonesian platform. A second alternative is that sea surface temperature changes at site 714A are out of phase with the Vostok pCO_2 record causing the seawater carbonate record to be different than expected. Finally, we cannot discount the possibility that cumulative errors associated with our calculations have made it difficult to resolve $[CO_3^{2-}]$ change sufficiently to map surface ocean carbonate chemistry to the ice core pCO_2 record.

7. FUTURE DIRECTIONS

This is the first attempt at reconstructing the surface $[CO_3^{2-}]$ for the glacial Indian Ocean. If the tropical Indian Ocean was periodically out of equilibrium with respect to atmospheric pCO_2, as our reconstruction suggests, than other parameters of the carbonate system should show similar oscillations. For instance, it should be possible to use

boron isotope measurements on *G. sacculifer* or *G. ruber* to determine whether surface pH fluctuated similarly (Sanyal *et al.*, 1996). Because the error on our $[CO_3^{2-}]$ reconstruction is large when only 10 shells/sample are analyzed (Table 2), the confidence limits around our estimates precludes further mechanistic discussions of the data set. At present we are addressing this and other issues by repeating the suite of isotope measurements on core 714A using a greater number of shells/sample and tightly constrained size fractions. A new suite of preliminary data indicate that the choice of shell size can have a considerable influence on reconstructed $\Delta[CO_3^{2-}]$ and $\Delta\delta^{13}C_{\Sigma CO2}$ (Mielke and Spero, unpublished data). Efforts to improve the application of these equations to the fossil record are continuing in our laboratories.

ACKNOWLEDGMENTS

We thank the staff of the University of Puerto Rico Isla Magueyes Marine Laboratory for their support during our field experiments. Thanks also to B. Bemis, C. Brogenski, J. Dailey, C. Fleschner, L. Juranek, H. Kurdi, K. Mielke, H. Sheene, and P. VonLangen for assistance in the laboratory during this project, S. Mulitza for comments on an earlier version of this manuscript and D. Rea for answering our eolian flux questions. Research support for this project was provided by the U.S. National Science Foundation (HJS, DWL and ADR) and Program for the Advancement of Special Research Projects at the Alfred Wegener Institute (JB).

9. REFERENCES

Anderson, O.R., and Bé, A.W.H., 1976. The ultrastructure of a planktonic foraminifera, *Globigerinoides sacculifer* (Brady), and its symbiotic dinoflagellates. J. Foram. Res., 6(1):1–21.

Archer, D., and Maier-Reimer, E., 1994. Effect of deep-sea sedimentary calcite preservation on atmospheric CO_2 concentration. Nature, 367:260–263.

Archer, D., Winguth, A., Lea, D., and Mahowald, N., in press. What caused the glacial/interglacial atmospheric PCO_2 cycles? Rev. Geophys.

Barnola, J.M., Raynaud, D., Korotkevich, Y.S., and Lorius, C., 1987. Vostok ice core provides 160,000-year record of atmospheric CO_2. Nature, 329:408–413.

Bé, A.W.H., 1977. An ecological, zoogeographic and taxonomic review of recent planktonic foraminifera. In: A.T.S. Ramsay (A.T.S. Ramsay), Oceanic Micropaleontology, Academic Press, London, 1–100.

Bé, A.W.H., 1980. Gametogenic calcification in a spinose planktonic foraminifer, *Globigerinoides sacculifer* (Brady). Mar. Micropaleontol., 5:283–310.

Bevington, P.R., 1969. Data reduction and error analysis for the physical sciences. McGraw-Hill, 336 pp.

Bijma, J., Hemleben, C., Huber, B.T., Erlenkeuser, H., and Kroon, D., 1998a. Experimental determination of the ontogenetic stable isotope variability in two morphotypes of *Globigerinella siphonifera* (d'Orbigny). Mar. Micropaleontol., 35(3–4):141–160.

Bijma, J., Hemleben, C., Oberhänsli, H., and Spindler, M., 1992. The effects of increased water fertility on tropical spinose planktonic foraminifers in laboratory cultures. J. Foram. Res., 22(3):242–256.

Bijma, J., Spero, H.J., and Lea, D.W., 1998b. Oceanic carbonate chemistry and foraminiferal isotopes: New laboratory results, Sixth Int. Conf. Paleoceanogr., Lisbon, Portugal, pp. 78.

Bijma, J., Spero, H.J., and Lea, D.W., 1999. Reassessing foraminiferal stable isotopes: Effects of seawater carbonate chemistry (experimental results), p. 489–512. In: G. Fischer, and G. Wefer (Editors), Use of Proxies in Paleoceanography: Examples from the South Atlantic. Springer-Verlag, Berlin.

Billups, K., and Spero, H.J., 1995. Relationship between shell size, thickness and stable isotopes in individual planktonic foraminifera from two equatorial Atlantic cores. J. Foram. Res., 25(1):24–37.

Boyle, E.A., 1992. Cadmium and $\delta^{13}C$ paleochemical ocean distributions during the stage 2 glacial maximum. Ann. Rev. Earth Planet. Sci., 20:245–287.

Broecker, W.S., 1982. Glacial to interglacial changes in ocean chemistry. Prog. Oceanogr., 11:151–197.

Broecker, W.S., and Henderson, G.M., 1998. The sequence of events surrounding Termination II and their implications for the cause of glacial-interglacial CO_2 changes. Paleoceanography, 13(4):352–364.

Broecker, W.S., and Peng, T.-H., 1987. The role of $CaCO_3$ compensation in the glacial to interglacial atmospheric CO_2 change. Global Biogeochemical Cycles, 1(1):15–29.

Broecker, W.S., and Peng, T.-H., 1998. Greenhouse Puzzles. Eldigio Press, New York, 277 pp.

Caron, D.A., Anderson, O.R., Lindsey, J.L., Faber, W.W.J., and Lim, E.L., 1990. Effects of gametogenesis on test structure and dissolution of some spinose planktonic foraminifera and implications for test preservation. Mar. Micropal., 16:93–116.

Clemens, S.C., and Prell, W.L., 1990. Late Pleistocene variability of Arabian Sea summer monsoon winds and continental aridity: Eolian records from the lithogenic component of deep-sea sediments. Paleoceanography, 5:109–145.

Crowley, T.J., 1995. Ice age terrestrial carbon changes revisited. Global Biogeochem. Cycles, 9(3):377–389.

Curry, W.B., and Crowley, T.J., 1987. The $\delta^{13}C$ of equatorial Atlantic surface waters: implications for ice age pCO_2 levels. Paleoceanography, 2(5):489–517.

Curry, W.B., Duplessy, J.C., Labeyrie, L.D., and Shackleton, N.J., 1988. Changes in the distribution of $\delta^{13}C$ of deep water ΣCO_2 between the last glaciation and the Holocene. Paleoceanography, 3(3):317–341.

Deuser, W.G., 1987. Seasonal variations in isotopic composition and deep-water fluxes of the tests of perennially abundant planktonic foraminifera of the Sargasso Sea: results from sediment-trap collections and their paleoceanographic significance. J. Foram. Res., 17(1):14–27.

Deuser, W.G., and Ross, E.H., 1989. Seasonally abundant planktonic foraminifera of the Sargasso Sea: Succession, deep-water fluxes, isotopic compositions, and paleoceanographic implications. J. Foram. Res., 19(4):268–293.

Droxler, A.W., Haddad, G.A., Mucciarone, D.A., and Cullen, J.L., 1990. Pliocene-Pleistocene aragonite cyclic variations in holes 714A and 716B (the Maldives) compared with hole 633A (the Bahamas): records of climate-induced $CaCO_3$ preservation at intermediate water depths. In: R.A. Duncan, J. Backman, L.C. Peterson *et al.* (Editors), Proceed. Ocean Drill. Progr. Sci. Res., pp. 539–577.

Duce, R.A. *et al.*, 1991. The atmospheric input of trace species to the world ocean. Global Biogeochem. Cycles, 5(3):193–259.

Duplessy, J.-C., Blanc, P.-L., and Bé, A.W.H., 1981. Oxygen-18 enrichment of planktonic foraminifera due to gametogenic calcification below the euphotic zone. Science, 213:1247–1250.

Duplessy, J.-C. *et al.*, 1988. Deepwater source variations during the last climatic cycle and their impact on the global deepwater circulation. Paleoceanography, 3(3):343–360.

Fairbanks, R.G., Sverdlove, M., Free, R., Wiebe, P.H., and Bé, A.W.H., 1982. Vertical distribution and isotopic fractionation of living planktonic foraminifera from the Panama Basin. Nature, 298:841–844.

Fairbanks, R.G., Wiebe, P.H., and Bé, A.W.H., 1980. Vertical distribution and isotopic composition of living planktonic foraminifera in the western North Atlantic. Science, 207:61–63.

Jouzel, J. *et al.*, 1993. Extending the Vostok ice-core record of paleoclimate to the penultimate glacial period. Nature, 364:407–412.

Kroopnick, P.M., 1985. The distribution of ^{13}C of ΣCO_2 in the world oceans. Deep-Sea Res., 32:57–84.

Lea, D.W., Bijma, J., Spero, H.J., and Archer, D., 1999. Implications of a carbonate ion effect on shell carbon and oxygen isotopes for glacial ocean conditions, p. 513–522. In: G. Fischer, and G. Wefer (Editors), Use of Proxies in Paleoceanography: Examples from the South Atlantic. Springer-Verlag, Berlin.

Lee, J.J., Freudenthal, H.D., Kossoy, V., and Bé, A., 1965. Cytological observations on two planktonic foraminifera, *Globigerina bulloides* d'Orbigny, 1826, and *Globigerinoides ruber* (d'Orbigny, 1839) Cushman, 1927. J. Protozool., 12(4):531–542.

Lohmann, G.P., 1995. A model for variation in the chemistry of planktonic foraminifera due to secondary calcification and selective dissolution. Paleoceanography, 10:445–457.

Martin, J.H., 1990. Glacial-interglacial CO_2 change: The iron hypothesis. Paleoceanography, 5(1):1–13.

Matsumoto, K., and Lynch-Stieglitz, J., 1999. Similar glacial and Holocene deep water circulation inferred from southeast Pacific foraminiferal carbon isotope composition. Paleoceanography, 14:149–163.

Murphy, P.P., Kelly, K.C., Feely, R.A., and Gammon, R.H., 1994. Carbon dioxide concentrations in surface water and the atmosphere: PMEL cruises 1986–1989. ERL PMEL-101, NOAA.

Peterson, L.C., and Prell, W.L., 1985. Carbonate preservation and rates of climatic change: An 800 kyr record from the Indian Ocean. In: E.T. Sundquist, and W.S. Broecker (Editors), The Carbon Cycle and Atmospheric CO_2: Natural Variations Archean to Present. American Geophysical Union, Washington D.C., pp. 251–269.

Ravelo, A.C., and Fairbanks, R.G., 1992. Oxygen isotopic composition of multiple species of planktonic foraminifera: Recorders of the modern photic zone temperature gradient. Paleoceanography, 7(6):815–831.

Sanyal, A., Hemming, N.G., Broecker, W.S., and Hanson, G.N., 1997. Changes in pH in the eastern equatorial Pacific across stage 5–6 boundary based on boron isotopes in foraminifera. Global Biogeochem. Cycles, 11(1):125–133.

Sanyal, A. *et al.*, 1996. Oceanic pH control on the boron isotopic composition of foraminifera: evidence from culture experiments. Paleoceanography, 11(5):513–517.

Sanyal, A., Hemming, N.G., Hanson, G.N., and Broecker, W.S., 1995. Evidence for a higher pH in the glacial ocean from boron isotopes in foraminifera. Nature, 373:234–236.

Schiffelbein, P., and Hills, S., 1984. Direct assessment of stable isotope variability in planktonic foraminifera populations. Palaeogeogr., Palaeoclimatol., Palaeoecol., 48:197–213.

Shackleton, N.J., 1977. Carbon-13 in Uvigerina: Tropical rainforest history and the equatorial Pacific carbonate dissolution cycles. In: N.R. Andersen, and A. Malahoff (Editors), The fate of fossil fuel CO_2 in the oceans. Plenum Publishing Corporation, New York, pp. 401–427.

Shackleton, N.J., Le, J., Mix, A., and Hall, M.A., 1992. Carbon isotope records from Pacific surface waters and atmospheric carbon dioxide. Quat. Sci. Rev., 11:387–400.

Spero, H.J., 1992. Do planktic foraminifera accurately record shifts in the carbon isotopic composition of sea water ΣCO_2? Mar. Micropaleontol., 19(1992):275–285.

Spero, H.J., Bijma, J., Lea, D.W., and Bemis, B.E., 1997. Effect of seawater carbonate concentration on foraminiferal carbon and oxygen isotopes. Nature, 390:497–500.

Spero, H.J., and Lea, D.W., 1993. Intraspecific stable isotope variability in the planktic foraminifera *Globigerinoides sacculifer*: Results from laboratory experiments. Mar. Micropaleontol., 22:221–234.

Spero, H.J., Lerche, I., and Williams, D.F., 1991. Opening the carbon isotope "vital effect" black box, 2: Quantitative model for interpreting foraminiferal carbon isotope data. Paleoceanography, 6:639–655.

Spero, H.J., and Williams, D.F., 1989. Opening the carbon isotope "vital effect" black box. 1. Seasonal temperatures in the euphotic zone. Paleoceanography, 4(6):593–601.

Takahashi, T. *et al.*, 1997. Global air-sea flux of CO_2: An estimate based on measurements of sea-air pCO_2 difference. Proc. Natl. Acad. Sci., 94:8292–8299.

Thunell, R.C., Curry, W.B., and Honjo, S., 1983. Seasonal variation in the flux of planktonic foraminifera: time series sediment trap results from the Panama Basin. Earth Planet. Sci. Lett., 64:44–55.

Tolderlund, D.S., and Bé, A.W.H., 1971. Seasonal distribution of planktonic foraminifera in the western North Atlantic. Micropaleontology, 17(3):297–329.